The EMBO Journal vol.12 no.10 pp.3729-3737, 1993

Residues within transmembrane segment M2 determine chloride conductance of glycine receptor homo- and hetero-oligomers

Joachim Bormann, Nils Rundström, Heinrich Betz and Dieter Langosch

Max-Planck-Institut für Hirnforschung, Deutschordenstrasse 46, 60528 Frankfurt/M. 71, Germany

Communicated by H.Betz

We have expressed glycine receptor (GlyR) α and β subunit cDNAs in HEK-293 cells to study the functional properties of homo- versus hetero-oligomeric GlyR channels. Dose-response curves of whole-cell currents in cells expressing α1 subunits revealed an average Hill coefficient of $h = 4.2$. Co-expression with the β subunit markedly increased glycine-gated whole-cell currents, which now exhibited a mean Hill coefficient of only $h = 2.5$. For α1, α2 and α3 homo-oligomers, the main-state single-channel conductances were 86, 111 and 105 pS, respectively, recorded at symmetrical Cl^- concentrations of 145 mM. The mutant α1 G221A gave rise to a main-state of 107 pS. This indicates that the main-state of α homo-oligomers depends on residue 221 which is located within transmembrane segment M2. Importantly, the main-state conductances of α1/β, α2/β and α3/β hetero-oligomers were only 44, 54 and 48 pS, respectively. The latter values are similar to those found in spinal neurons, suggesting that native GlyRs are predominantly α/β hetero-oligomers. Co-expression of α1 with mutant β subunits revealed that residues within and close to segment M2 of the β subunit determine the conductance differences between homo- and hetero-oligomers.

Key words: chloride channel/glycine receptor/M2 segment

Introduction

The glycine receptor (GlyR) is a ligand-gated ion channel protein mediating synaptic inhibition in spinal cord and other brain regions. The GlyR counteracts excitatory membrane depolarization by increasing the Cl^- permeability of the postsynaptic membrane (see Betz, 1992). The mechanism of ion flux through GlyR channels has been analyzed by applying patch-clamp techniques to cultured mouse spinal neurons and slices. Accordingly, the glycine-gated channel is an anion-selective pore of 0.52 nm in diameter, which contains internal binding sites for permeating Cl^- ions and adopts an elementary main-state conductance of 42-48 pS plus a number of other conductance states (Hamill *et al.*, 1983; Bormann *et al.*, 1987; Smith *et al.*, 1989; Bormann, 1991; Takahashi and Momiyama, 1991; Twyman and MacDonald, 1991; Takahashi *et al.*, 1992).

Biochemical analysis of affinity-purified GlyR preparations revealed a pentameric arrangement of α (48 kDa) and β (58 kDa) subunits (Pfeiffer *et al.*, 1982; Langosch *et al.*, 1988). Both polypeptides share significant sequence homology and a common predicted transmembrane topology including four transmembrane segments (M1-M4) with subunits of nicotinic acetylcholine (nAChR) and γ-aminobutyric acid receptors ($GABA_AR$) (Grenningloh *et al.*, 1987, 1990a). Within GlyR polypeptides, the known isoforms of the 48 kDa subunit (α1-α3) display an overall amino acid identity of 82%. The β subunit diverges from the α subunits, showing an average identity of only 48% to the former (Grenningloh, 1990b). Expression of α subunits in *Xenopus* oocytes or human embryonic kidney cells (HEK-293 cells) results in the formation of glycine-gated chloride channels, which are blocked by strychnine and picrotoxinin (Schmieden *et al.*, 1989; Sontheimer *et al.*, 1989; Grenningloh *et al.*, 1990a; Kuhse *et al.*, 1990). Upon co-expression of α and β subunits, picrotoxinin-insensitive α/β hetero-oligomers are formed. Based on site-directed mutagenesis, the picrotoxinin binding site was assigned to the M2 segment of the α subunit (Pribilla *et al.*, 1992). As picrotoxinin is commonly regarded as a chloride channel blocker, this suggests that the M2 segment contributes to the wall of the GlyR pore in analogy to other ligand-gated ion channels (Imoto *et al.*, 1988, 1991; Villarroel *et al.*, 1992). Also, a synthetic peptide corresponding to the M2 segment of the α1 subunit has been demonstrated to form ion channels upon incorporation into planar bilayers (Langosch *et al.*, 1991).

In situ hybridization studies indicate a widespread expression of GlyR α and β subunit mRNAs in the mammalian CNS (Malosio *et al.*, 1991; Betz, 1992). The various α subtypes are expressed in regionally and temporally distinct patterns. Whereas α1 transcripts found in spinal cord and brain stem increase during development, α2 transcripts decrease from high prenatal to low adult levels and α3 transcripts are of low abundance at all developmental stages. β Subunit transcripts are abundant in most CNS regions throughout development. To study the functional properties of different GlyR subunit combinations, we expressed α and β subunits in mammalian cells, and characterized the resulting homo- and hetero-oligomeric channels. Our results demonstrate that hetero-oligomeric GlyRs exhibit functional properties corresponding to native GlyR in spinal cord neurons. Expression of mutant subunits identified amino acid residues within segment M2 as determinants of Cl^- conductance of homo- and hetero-oligomeric receptor channels.

Results

To compare homo-oligomeric GlyRs composed of one type of α subunit (α1-α3) with hetero-oligomeric α/β receptors, we studied: (i) the magnitude, glycine concentration dependence and Cl^- selectivity of whole-cell currents and (ii) the unitary conductance of wild-type and mutant receptor channels generated by heterologous expression.

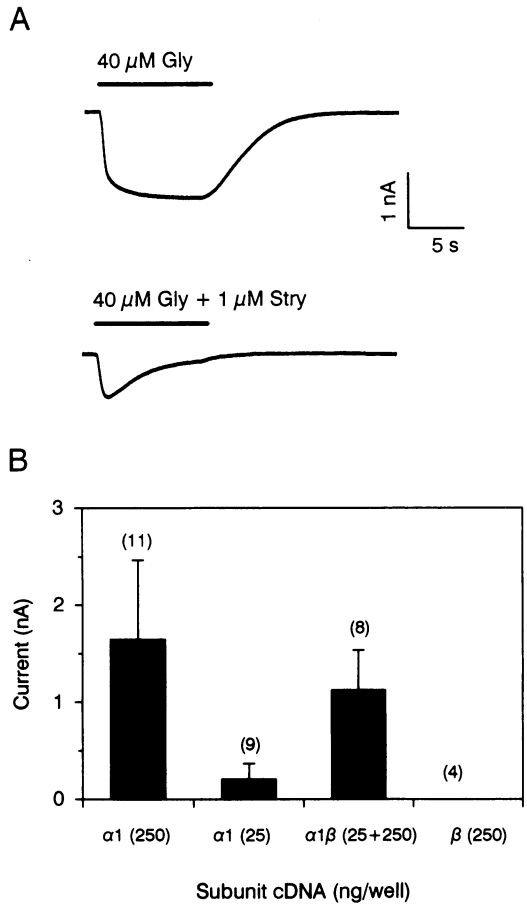

Fig. 1. Functional expression of homo- and hetero-oligomeric GlyRs in HEK-293 cells. (**A**) Whole-cell current induced in cells transfected with 250 ng α1 cDNA. Application of 40 μM glycine (Gly) gives rise to an inward current, which results from the outwardly directed movement of Cl^- ions (top). The cell was recorded with intra- and extracellular Cl^- of 145 mM and clamped at −70 mV holding potential. Upon co-application of 1 μM strychnine (Stry), the glycine response showed an initial peak, which rapidly declined to almost baseline level (bottom). (**B**) Co-expression of α and β subunits. Cells were transfected with various amounts of α1 and β cDNAs. Numbers denote ng cDNA/coverslip. Average whole-cell currents induced by 40 μM glycine are plotted (±SD) on the ordinate. In cells transfected with α1 alone, the current strongly depended on the cDNA dose. With β cDNA alone, no measurable response was recorded. Upon co-expression of a low dose of α1 (25 ng) plus a 10-fold excess of β cDNA, currents were markedly elevated as compared to the average response obtained with 25 ng α1 cDNA alone.

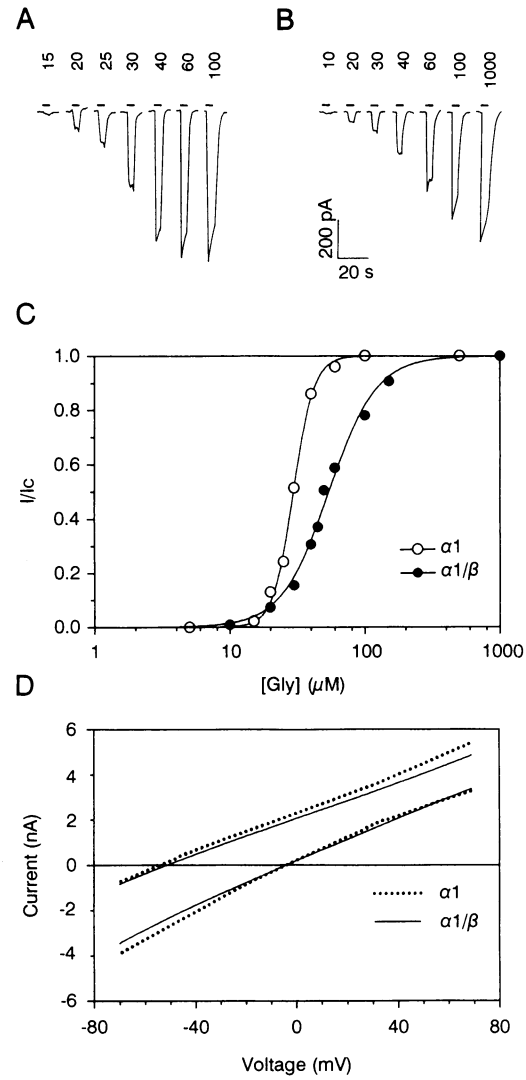

Fig. 2. Agonist-response behavior and Cl^- selectivity of homo- or hetero-oligomeric GlyRs. (**A**–**C**) Concentration dependence of glycine-induced whole-cell currents recorded in cells transfected with α1 (A) or α1 plus β (1:10) cDNAs (B). The numbers above the application bars denote glycine concentration in μM. Dose–response curves (C) of peak currents (I) were normalized to the value obtained at 1000 μM glycine (I_c). The sigmoidal curves are fits to the Hill equation, $I/I_c = C^h/C^h + EC_{50h}$, where I/I_c represents normalized current, EC_{50} the glycine concentration eliciting the half-maximal response, C glycine concentration, and h the Hill coefficient. Open and closed symbols correspond to α1 (A) and α1/β channels (B), respectively. From the fits to the data illustrated in A and B, EC_{50} values are 30 and 54 μM glycine, and the Hill coefficients 5.7 and 2.5 for α1 and α1/β channels, respectively. (**D**) Cl^- selectivity of α1 and α1/β channels. Current–voltage relationships of glycine-induced whole-cell currents were measured by ramping the membrane potential from −70 to 70 mV (100 mV/s). Dotted and solid lines indicate α1 and α1/β channels, respectively. The right-hand pair of traces was obtained at symmetrical Cl^- concentrations of 145 mM and intersects the voltage axis at ~0 mV. Upon replacing 125 mM of the intracellular Cl^- by the impermeant anion gluconate, the reversal potential was shifted to −54 mV for α1 and −51 mV for α1/β channels (left-hand pair).

Expression of homo- and hetero-oligomeric GlyRs

Transfection of HEK-293 cells with α1, α2 or α3 subunit cDNAs resulted in the formation of functional homo-oligomeric channels, which were studied by whole-cell recording. As these cells are known to form electrically coupled clusters (Sontheimer *et al.*, 1989), care was taken to record from lone cells not in contact with neighbor cells. The fast application of 40 μM glycine to cells at −70 mV holding potential induced strychnine-sensitive inward currents (Figure 1A), which were generally larger for cells transfected with 250 ng α1 cDNA/coverslip (1650 ± 813 pA, mean ± SD, n = 11 cells, Figure 1B) as compared to cells transfected with the same amounts of α2 (441 ± 139 pA, n = 9) or α3 cDNA (328 ± 114 pA, n = 4) (not illustrated). Co-expression of α subunits with the β subunit significantly enhanced glycine-induced whole-cell currents. Figure 1B shows the results for the α1/β combination when a 10-fold excess of β over α cDNA was used for transfection. The average whole-cell current recorded with 25 ng α1 cDNA plus 250 ng β cDNA/coverslip (1128 ± 406 pA, n = 8) was ~5 times larger than that obtained with 25 ng α1 cDNA alone (213 ± 155 pA, n = 9) in a parallel experiment. The β subunit (250 ng cDNA) alone did not

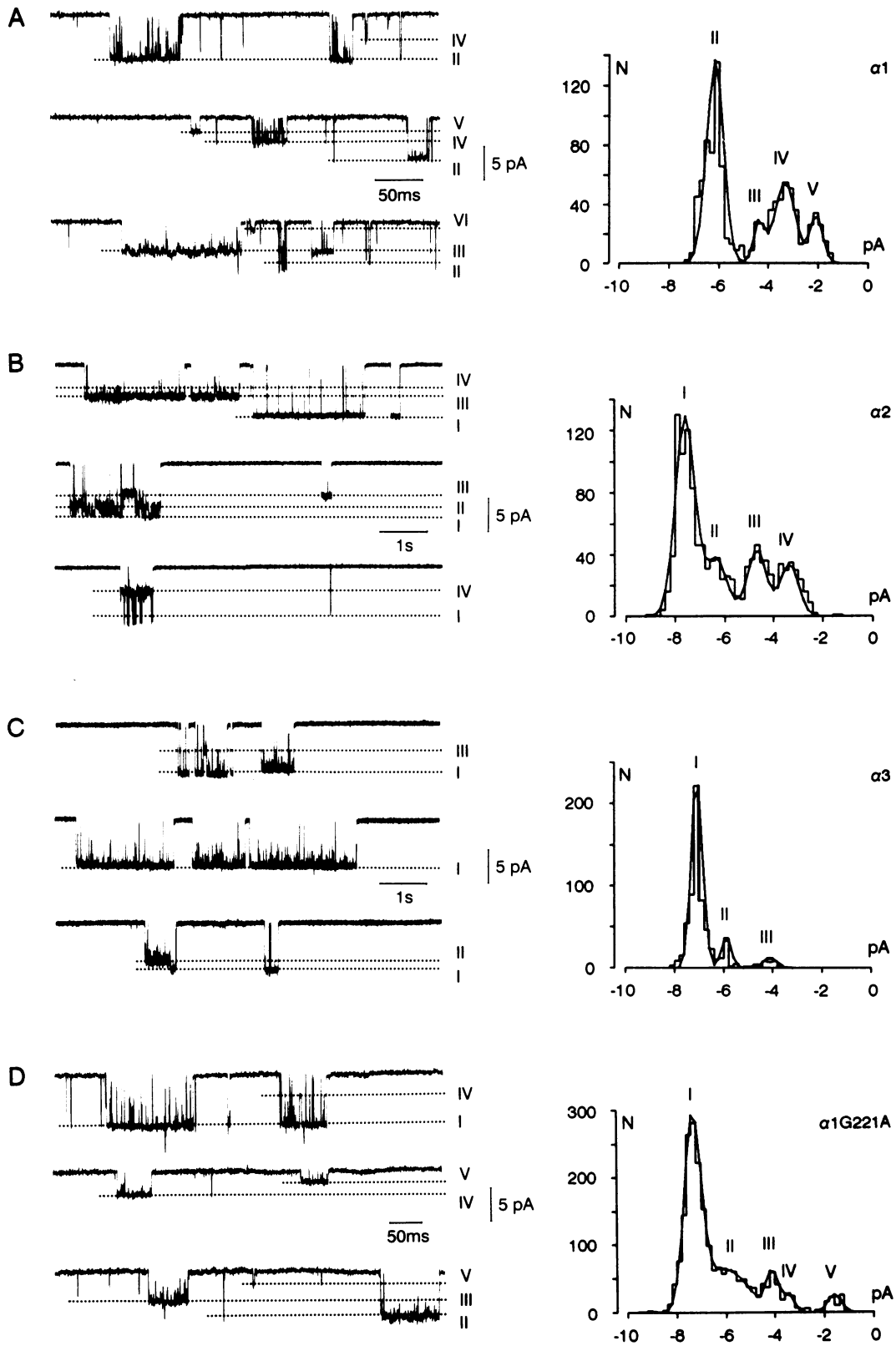

Fig. 3. Conductance states of α homo-oligomeric GlyRs. Single-channel currents (left) were recorded from outside-out patches at −70 mV membrane potential. The conductance levels are marked by dotted lines and labeled by Roman numerals which correspond to the peaks in the amplitude histograms (right). Distributions were fitted by multiple Gauss functions (solid lines), which yield the relative percentage of conductance states. (**A**) α1 channels with conductance levels of 88 pS (II, 55%), 68 pS (III, 7%), 48 pS (IV, 28%) and 30 pS (V, 10%). In addition, a small and infrequent conductance state of 18 pS (VI) is seen which does not appear in the histogram. (**B**) α2 channels with conductance levels of 109 pS (I, 53%), 90 pS (II, 16%), 67 pS (III; 18%) and 48 pS (IV, 13%). (**C**) α3 channels with conductance levels of 102 pS (I, 87%), 85 pS (II, 10%) and 58 pS (III, 3%). (**D**) α1G221A channels with conductance states of 105 pS (I, 59%), 86 pS (II, 28%), 59 pS (III, 7%), 45 pS (IV, 3%) and 25 pS (V, 3%). Main-state conductances in these patches were 88, 109, 102 and 105 pS for A, B, C and D, respectively. Traces were filtered at 2.3 kHz (−3 dB) (A,D) or 0.5 kHz (−3 dB) (B,C).

form detectable channels under these conditions. The elevated whole-cell currents seen upon co-expression indicate that α and β subunits co-assemble and thus increase the total number of functional GlyR channels in the plasma membrane. Qualitatively similar effects were found upon co-expression of $\alpha 2$ or $\alpha 3$ subunits with β (not shown).

Agonist-response properties

Whole-cell currents through homo-oligomeric GlyR channels showed a steep dependence on external glycine concentration (Figure 2A and C). For $\alpha 1$ channels, the average glycine concentration required for half-maximal activation (EC_{50}) was 39 ± 17 μM (mean ± SD, n = 22 cells) and the mean Hill coefficient h = 4.2 ± 1.6 (Figure 2C). This implies that at least five glycine molecules must bind to activate homo-oligomeric glycine receptors. With $\alpha 1/\beta$ hetero-oligomers, an EC_{50} value of 48 ± 17 μM (n = 29), similar to that of $\alpha 1$ homo-oligomers, was found. Importantly, the average Hill coefficient was only h = 2.5 ± 0.9 for $\alpha 1/\beta$ hetero-oligomers (Figure 2B and C); this value is significantly lower than that of $\alpha 1$ channels (P = 0.0001, Student's t-test). This suggests that three glycine molecules are sufficient to activate $\alpha 1/\beta$ hetero-oligomers.

Cl^- selectivity

The ion selectivity of $\alpha 1$ channels was compared to that of $\alpha 1/\beta$ hetero-oligomers by measuring the current–voltage (I–V) relationships of glycine-induced whole-cell currents at different Cl^- gradients across the cell membrane. When the voltage was ramped from −70 to 70 mV with Cl^- present at 145 mM at both membrane faces, the current polarity reversed from inward to outward at ~0 mV with either homo- or hetero-oligomers (Figure 2D). Upon partial substitution of Cl^- in the intracellular solution by the larger anion gluconate, the reversal potentials were shifted to more negative values as expected for Cl^- selective channels (Figure 2D). With 25 mM Cl^- inside and 145 mM Cl^- outside the cell, average reversal potentials of −46 ± 7 mV (n = 5 cells) were obtained for $\alpha 1$ and −48 ± 3 mV (n = 3 cells) for $\alpha 1/\beta$ channels. Similar values were obtained with $\alpha 2$ and $\alpha 3$ channels (data not shown). These reversal potentials are close to those predicted by the Nernst equation (−49 mV). Hence, homo- and hetero-oligomeric GlyR channels share strong selectivity for permeating Cl^- ions.

Conductance of homo-oligomeric α channels

To investigate elementary conductances, we recorded from single channels in outside-out patches isolated from cells transfected with different α subunits. At −70 mV and with 145 mM Cl^- on both membrane faces, glycine-activated elementary inward currents with a predominant amplitude of ~6 pA were observed (Figure 3). The current–voltage (i–V) relationships measured between −90 and 50 mV reversed at ~0 mV (Figure 6A). Average main-state conductances were different for $\alpha 1$ and $\alpha 2/3$ subunits: $\alpha 1$, 86 ± 1 pS (mean ± SD, n = 7 patches); $\alpha 2$, 111 ± 2 pS (n = 5); $\alpha 3$, 105 ± 11 pS (n = 7) (Figure 3, conductance states I and II). In addition, smaller and less frequent conductances were observed for each receptor type (summarized in Table I). Albeit these minor states usually occurred as separate events, direct transitions between different conductance levels were seen within bursts of

Table I. Conductance states of homo- and hetero-oligomeric GlyRs

	N	I	II	III	IV	V	VI
$\alpha 1$	7	–	86 ± 1 (7) 71%	64 ± 2 (6) 9%	46 ± 2 (6) 15%	30 ± 2 (4) 5%	18 (2) <0.1%
$\alpha 2$	5	111 ± 2 (5) 57%	91 ± 1 (3) 7%	66 ± 2 (4) 18%	48 ± 1 (3) 14%	36 ± 2 (3) 4%	23 (2) <0.1%
$\alpha 3$	7	105 ± 11 (7) 60%	85 ± 7 (6) 23%	62 ± 6 (6) 14%	42 (2) 2%	30 (1) 0.3%	20 (1) 0.6%
$\alpha 1$G221A	5	107 ± 7 (5) 58%	91 ± 7 (5) 16%	67 ± 8 (5) 9%	47 ± 3 (4) 15%	26 ± 1 (4) 2%	–
$\alpha 1/\beta$	6	–	–	–	44 ± 5 (6) 88%	29 ± 3 (3) 5%	20 ± 4 (5) 7%
$\alpha 2/\beta$	6	112 ± 9 (4) 11%	80 (1) 1%	–	54 ± 4 (6) 74%	36 ± 5 (6) 14%	–
$\alpha 3/\beta$	3	–	–	–	48 ± 2 (3) 72%	34 ± 1 (3) 21%	23 (2) 7%
$\alpha 1/\beta$E290Q	6	–	–	58 ± 8 (3) 29%	46 ± 2 (6) 58%	30 ± 4 (5) 12%	19 (2) 1%
$\alpha 1/\beta$B	5	–	95 (1) 10%	–	53 ± 4 (5) 60%	36 ± 4 (5) 28%	20 (1) 2%
$\alpha 1/\beta$E297S	5	–	98 (2) 23%	70 (2) 2%	50 ± 1 (3) 30%	35 ± 1 (3) 42%	19 (2) 3%
$\alpha 1/\beta$E290Q,E297S	8	–	94 ± 5 (6) 18%	77 (2) 6%	54 ± 5 (8) 66%	30 ± 5 (6) 10%	–
$\alpha 1/\beta$B,E297S	7	–	87 ± 9 (7) 81%	73 ± 5 (7) 15%	52 ± 6 (3) 3%	30 (2) 1%	–

GlyRs were activated in outside-out patches by 1–10 μM glycine. Conductance states are denoted by Roman numerals (I–VI). Mean conductance values ± SD are given in pS, together with the number of patches (in parentheses) where a particular state was observed. Main-state conductance is underlined. Percentage numbers indicate the relative frequency for each conductance state. The total number of patches (N) is given for each GlyR studied.

openings. Therefore, the different conductances seen with any one receptor type are likely to arise from the same channel. Notably, a conductance (91 and 85 pS) comparable to the main-state of α1 channels (state II) appeared as a minor state with α2 and α3 channels, respectively. We propose that the larger main-state conductance (state I) of α2/α3 channels is an additional conductance not accessible to α1 channels.

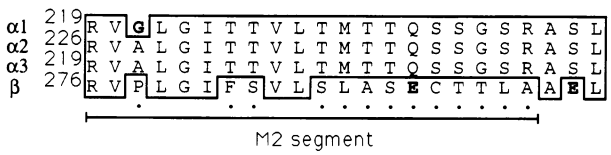

Fig. 4. Alignment of the M2 segments of GlyR α1−α3 and β subunits. Identical amino acids are boxed. Bold-face letters indicate the positions of mutated amino acids in α1 or β subunits (α1G221A, βE290Q, βE297S). Residues that were exchanged within the β chain for the corresponding residues of the α1 subunit to yield mutant βB (Pribilla *et al.*, 1992) are indicated by dots.

To elucidate the structural basis for the different main-state conductances of α1 versus α2/α3 homo-oligomers, we mutated glycine 221 of the α1 chain into an alanine. This is the only residue not conserved within the respective transmembrane segments M2 (Figure 4), which are implicated in forming the GlyR pore (Pribilla *et al.*, 1992). Mutant α1G221A exhibited a main-state conductance of 107 ± 7 pS (58% of all events, $n = 5$) similar to state I of α2/α3 channels (Figure 3) and a linear i−V relationship (Figure 6A). The α1 main-state (state II) appeared as a subconductance (91 ± 7 pS) at minor frequency (16%) with the mutant (Table I). We thus infer that the main-state of α1G221A corresponds to the α2/3 conductance and extends the conductance repertoire of α1 channels.

Conductance of α/β hetero-oligomers

For single-channel analysis of hetero-oligomers, we recorded from outside-out membrane patches of cells transfected with a 10-fold excess of β over α cDNA to minimize the

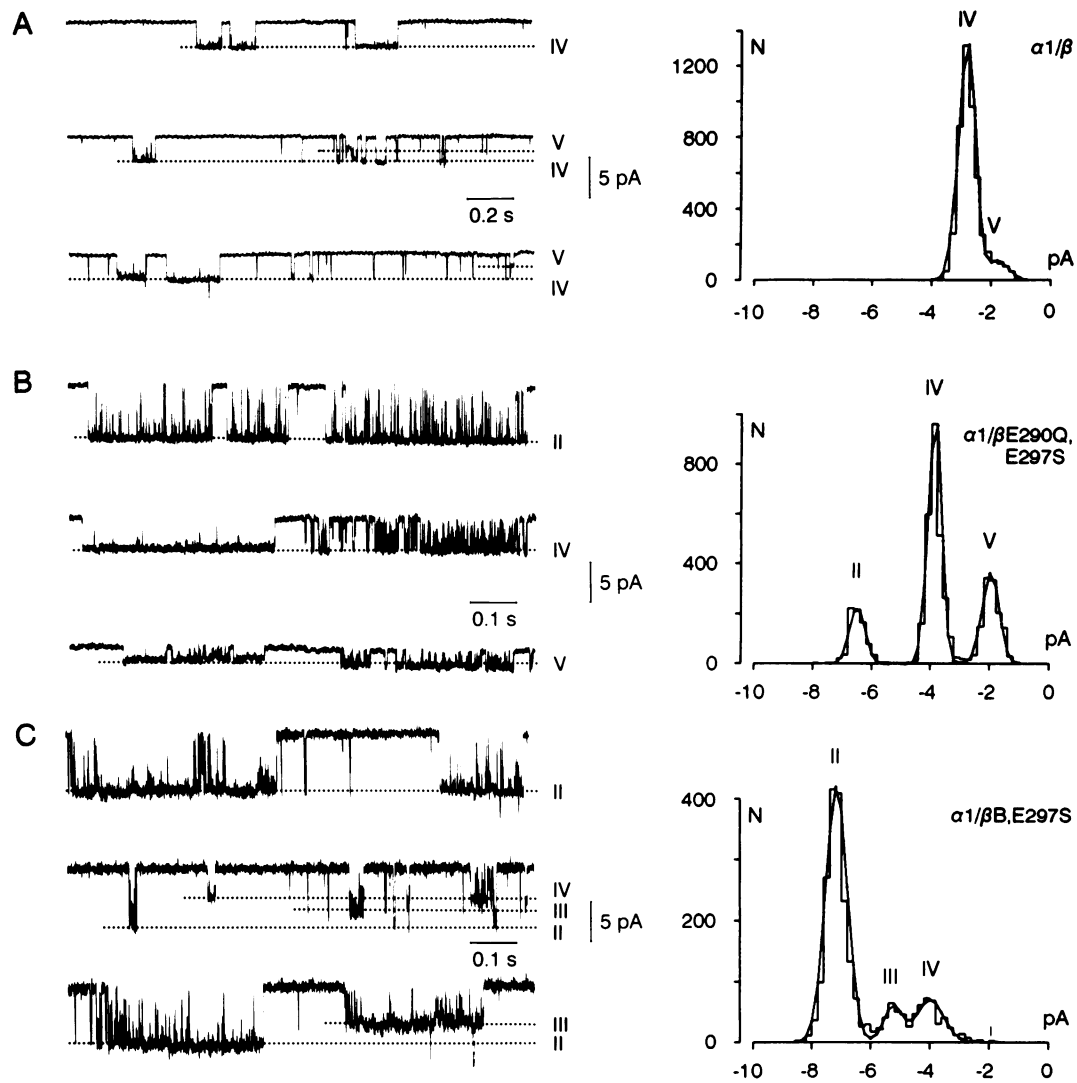

Fig. 5. Conductance states of hetero-oligomeric GlyRs in outside-out patches. (**A**) α1/β channels with conductance states of 41 pS (IV, 85%) and 31 pS (V, 15%). (**B**) α1/βE290Q,E297S channels with conductance states of 93 pS (II, 19%), 55 pS (IV, 55%) and 28 pS (V, 26%). (**C**) α1/βB,E297S channels with conductance states of 102 pS (II, 75%), 75 pS (III, 16%) and 57 pS (IV, 9%). The main-state conductances in these patches were 41, 55 and 102 pS for A, B and C, respectively. (**C**) α1/βB,E297S channels with conductance states of 102 pS (II, 75%), 75 pS (III, 9%) and 57 pS (IV, 16%), respectively. An interesting functional difference was noted between α or α/β and α/β mutant channels. Whereas the different conductances of wild-type channels occurred alternatingly, they tended to cluster within individual bursts of α/β mutant channels. Traces were filtered at 0.5 kHz (−3 dB) (A) or 2.3 kHz (−3 dB) (B,C).

formation of α homo-oligomers. According to the amplitude histograms shown in Figure 5 and the data in Table I, the main-state conductances for α1/β, α2/β and α3/β channels were 44 ± 5 pS (n = 6), 54 ± 4 pS (n = 6) and 48 ± 2 pS (n = 3), respectively. These conductances correspond roughly to conductance state IV of α homo-oligomers. In addition, each α/β combination exhibited several smaller conductance states (states V and VI) which, however, were occupied more frequently as compared to α channels (Table I). The i−V relationship for the α1/β main-state was linear between −90 and 50 mV, and revealed a reversal potential near 0 mV (Figure 6B). As the main-state conductances are much lower than those of the corresponding α homo-oligomers, it appears that the selection of the main-state depends on the presence of the β subunit. Channels corresponding to the main-states of α1 or α3 homo-oligomers were virtually absent under these conditions. Only with the α2/β combination were state I and II conductances observed at a significant frequency; presently, we cannot decide whether these are an intrinsic property of α2/β channels or whether they arise from contaminating α2 homo-oligomers. The predominant conductance values of α/β hetero-oligomers are reminiscent of those of native GlyRs recorded earlier in spinal cord neurons (42−48 pS main-state; Hamill *et al.*, 1983; Bormann *et al.*, 1987; Smith *et al.*, 1989; Takahashi and Momiyama, 1991; Twyman and MacDonald, 1991; Takahashi *et al.*, 1992), suggesting that native GlyRs are composed of both types of subunits.

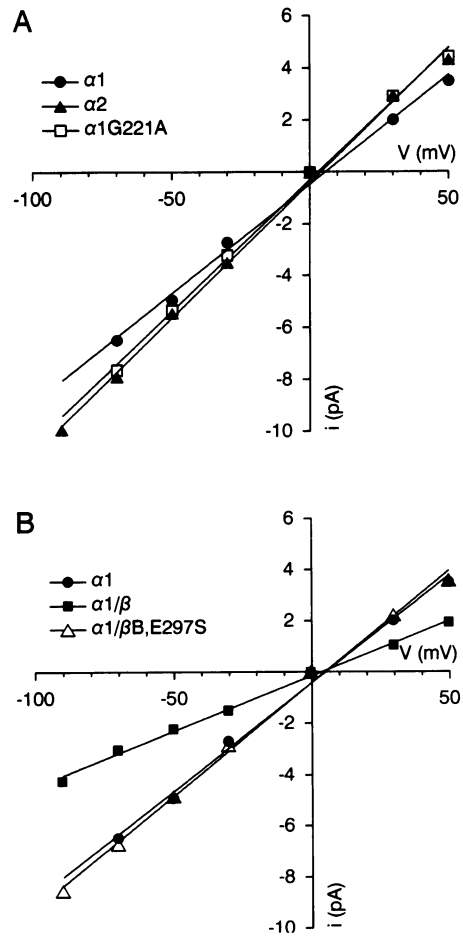

Fig. 6. i−V relationships of wild-type and mutant GlyR main-state conductances. Single-channel currents were measured in the voltage range from −90 to 50 mV and fitted by straight lines. (**A**) Effect of α1G221A mutation. α1 (●) and α2 channels (▲) revealed main-state conductances of 86 and 104 pS, respectively. The mutant α1G221A (□) had a main-state of 101 pS, very close to that of α2 channels. (**B**) Effect of β mutation. α1 (●) and α1/β (□) channels displayed main-states of 86 and 43 pS, respectively. α1 co-expressed with the mutant βB,E297S reveals a main-state conductance of 88 pS (△), virtually indistinguishable from that of α1 channels.

In order to delineate those amino acids responsible for the difference in conductance between α and α/β channels, we co-expressed the α1 subunit with β chains mutated within and close to its M2 segment (see Figure 4). Channels composed of the α1 subunit and mutant βE290Q, where the glutamate residue located within the M2 segment was replaced by glutamine, the respective residue of the α chain, showed an additional subconductance of 58 ± 8 pS (n = 3) equivalent to state III of α channels (Table I). Yet a larger substate similar to the α1 main-state (state II, 98 pS, n = 2) was seen with mutant βB, albeit in one patch only. For construction of βB, residues 278−295, i.e. the whole M2 segment, were exchanged by the corresponding α1 sequence (see Pribilla *et al.*, 1992). With βE297S, where a glutamate C-terminal to the M2 segment was substituted for serine, subconductances corresponding to both state II (98 pS, n = 2) and state III (70 pS, n = 2) were seen. A similar picture emerged with the double mutant βE290Q,E297S (94 ± 5 pS, n = 6 and 77 pS, n = 2; Figure 5B). The most pronounced effect was observed when the mutation E297S was introduced into mutant βB. Now, a conductance corresponding to state II (87 ± 9 pS) constituted the main-state (81% of all events) of the hetero-oligomers (Figure 5C). Like the α1/β main-state, this conductance was characterized by a linear i−V relationship (Figure 6B).

Thus, hetero-oligomers of α1 with β subunits carrying multiple substitutions between positions 278 and 297 display a range of conductances very similar to α1 homo-oligomers. Residues within and C-terminal to the M2 segment, therefore, determine the difference in the conductance patterns displayed by α1 and α1/β channels.

Discussion

Our results demonstrate distinct functional differences between recombinant α homo- and α/β hetero-oligomeric GlyR isoforms. Differences found between elementary conductances could be largely attributed to amino acids at the presumed channel-forming regions. Further inferences can be made about the subunit composition of native GlyRs.

Functional properties of recombinant GlyR channels

Whole-cell recording confirmed the efficient formation of anion-selective homo-oligomeric GlyRs previously found upon expression of α1, α2 or α3 subunits in *Xenopus* oocytes (Schmieden *et al.*, 1989; Grenningloh et al., 1990a; Kuhse *et al.*, 1990) and in HEK-293 cells (Sontheimer *et al.*, 1989). We did not observe currents in cells expressing the β subunit alone at glycine concentrations up to 0.5 mM. This is consistent with previous findings, where very high glycine concentrations (EC_{50} = 24 mM) elicited only small inward currents in *Xenopus* oocytes nuclearly injected with β subunit cDNA (Grenningloh *et al.*, 1990b). Apparently, the β subunit carries only a very low-affinity glycine site and/or does not assemble efficiently into functional channels. However, co-expression of GlyR α and β subunits strongly

increased glycine-gated whole-cell currents. This suggests the efficient formation of α/β hetero-oligomeric GlyRs, and is in line with earlier results where co-expressed α and β subunits could be co-immunoprecipitated and exhibited a drastically diminished picrotoxinin sensitivity as compared to α homo-oligomers (Pribilla *et al.*, 1992). Co-assembly of α with β subunits may increase the total number of functional channels in the plasma membrane by (i) the higher number of subunits available for complex formation and/or (ii) a more efficient targeting of α/β complexes to the cell's plasma membrane as compared to α homo-oligomers. The latter interpretation is based on the concept that oligomerization of newly synthesized membrane protein subunits occurs in the endoplasmic reticulum and is followed by transport of assembled receptors via Golgi compartments to the plasma membrane (Hurtley and Helenius, 1989). For example, it has been shown for the structurally related nAChR that individually expressed β, γ or δ subunits are retained in intracellular compartments; only upon co-expression with the α subunit are functional hetero-oligomeric nAChRs found in the plasma membrane (Claudio *et al.*, 1989). As the increase in current observed upon GlyR α/β co-expression is higher than expected from the higher number of available subunits, a similar situation may pertain to the GlyR.

The Hill coefficients as found in this study for $\alpha 1$ homo-oligomers ($h = 4.2$) were significantly higher than the values reported earlier for oocytes ($h = 3$, Schmieden *et al.*, 1989) and HEK-293 cells ($h = 2$, Sontheimer *et al.*, 1989). This discrepancy may be explained by the slower speed of glycine application in the latter studies which may have distorted dose–response curves due to receptor desensitization at higher agonist concentrations (Akaike and Kaneda, 1989). The Hill coefficients determined here imply that at least five agonist molecules bind to activate the channels, consistent with a pentameric structure of α homo-oligomeric channels, where each subunit provides a glycine binding site (Sontheimer *et al.*, 1989). Importantly, a significantly lower Hill coefficient was seen with $\alpha 1/\beta$ channels ($h = 2.5$). This suggests that three agonist molecules are sufficient to activate α/β hetero-oligomers.

Role of residue $\alpha 1$ G221

Single-channel recording revealed different main-state conductances for each α homo-oligomer (86, 111 and 105 pS for $\alpha 1$, $\alpha 2$ and $\alpha 3$ channels) which were acccompanied by a variety of less frequently occurring smaller conductances. These conductance states are similar, but not identical, to values reported recently for $\alpha 1$ and $\alpha 2$ channels analyzed in *Xenopus* oocytes (75 and 88 pS for $\alpha 1$ and $\alpha 2$, respectively; Takahashi *et al.*, 1992). It remains to be seen whether these differences can be attributed to the different expression systems used.

An important point is that the main-state conductance of $\alpha 1$ channels (state II) is preserved as a minor conductance state with $\alpha 2/\alpha 3$ channels. This suggests that the higher $\alpha 2/\alpha 3$ main-states (state I) represent a conductance beyond the repertoire of $\alpha 1$ channels. Interestingly, the main-state conductance of the mutant α1G221A, whose transmembrane sequence M2 is identical to that of $\alpha 2/\alpha 3$ chains, was similar to that of $\alpha 2/3$ channels, while the $\alpha 1$ main-state again appeared at lower frequency. This supports the earlier notion that the Cl^- pore of the GlyR is lined by its subunit's M2 domains (Langosch *et al.*, 1991; Pribilla *et al.*, 1992). Sequence alignments between different ligand-gated ion channel subunits (see Pribilla *et al.*, 1992) predict that residue G221 is exposed to the lumen of the GlyR's Cl^- channel. For nAChR channels, the equivalent position was inferred to be the most constricted site as introducing larger side chains resulted in a reduced conductance (Imoto *et al.*, 1991; Villaroel *et al.*, 1992). Adding a methyl side chain at this position of the M2 segment of the GlyR channel did not, however, reduce ion flow. Rather, it forced the mutant to adopt the higher $\alpha 2/\alpha 3$ main-state conductance in addition to the conductances seen with $\alpha 1$ channels. We suggest that this side chain exerts a conformational rather than a steric effect.

Role of residues in the β M2 segment

Upon co-expression of different α/β combinations, the main-state conductances were only 44–54 pS and the substates 29–36 and 20–23 pS, respectively. The relative frequencies of the different conductance states did not appear to depend on the glycine concentrations (1–10 μM) applied to elicit channel activity in different patches. This conductance repertoire corresponds to a subset of α channel conductances including states IV–VI. It suggests that incorporation of the β subunit into the channel complex preferentially stabilizes the lower conductance states and hinders activation of the larger states I–III seen with α homo-oligomers.

By co-expressing $\alpha 1$ with β subunits mutated at the channel-forming M2 segment (Pribilla *et al.*, 1992), we identified amino acid positions determining the range of conductances accessible to α/β channels. Upon exchanging βE290Q within segment M2, a conductance similar to state III of α homo-oligomers was added to the subset of $\alpha 1/\beta$ channels. Yet a larger substate of state II was added upon exchange βE297S at a position C-terminal to M2 and predicted to reside at the extracellular mouth of the GlyR channel. This substate was also occasionally seen with mutant βB whose M2 segment was made identical to the $\alpha 1$ chain by an exchange of 13 residues. With the double mutant βE290Q,E297S, the distribution of conductances was similar to βE297S. A very pronounced effect was, however, observed when the mutation E297S was introduced into the βB mutant. Now, the state II conductance (87 pS) appeared as the main-state; $\alpha 1/\beta$B,E297S channels thus behaved very similarly to $\alpha 1$ homo-oligomers. In conclusion, it appears that the mutation βE297S is the most critical one allowing for state II and III conductances; however, preferential activation of state II is observed only upon fully interconverting the M2 sequence of the β subunit into that of the $\alpha 1$ chain.

It is tempting to speculate that the pivotal role of residues βE290 and βE297 is related to electrostatic repulsion between their negatively charged side chains and permeating Cl^- ions. However, their presence appears to affect only state I–III, but not state IV–VI conductances. Thus, an electrostatic effect may be discussed in the context of a mechanism governing substate selection. As direct transitions between different conductance states were observed, they are likely to arise from the same channel and may correspond to different conformations of the ion pore. We speculate that those conformations corresponding to state I–III conductances also exist with α/β hetero-oligomeric channels; however, the glutamate side chains of the β subunit may be exposed such that electrostatic barriers for Cl^- ions are formed with the latter states. Consequently, these

conformations would yield inactive α/β channels. As these negative charges are removed in the $\alpha1/\beta$ mutant combinations, the same conformations there would allow passage of Cl^- ions at rates corresponding to states II and III of $\alpha1$ homo-oligomers. In other words, this model would imply that an unfavorable interaction of negatively charged residues with anions precludes activation of certain conductance states.

A regulation of channel conductance by charged side chains has been demonstrated for several other systems. Exchanges of glutamate or aspartate residues bordering the M2 segment reduced the cation current through the nAChR channel (Imoto *et al.*, 1988) to extents depending on the distance of the respective residues from the most constricted channel site (Villarroel *et al.*, 1992). Similarly, multiple substitutions including a glutamate–alanine exchange at the N-terminus of M2 are required to convert the cation channel of the $\alpha7$ nAChR into an anion-selective pore, i.e. the presence of a glutamate appears to be incompatible with anion permeation (Galzi *et al.*, 1992). On the other hand, the introduction of a positively charged arginine residue into the M2 segment of glutamate receptor subunit D drastically diminished the inward flow of cations (Verdoorn *et al.*, 1991). These observations may be generally interpreted such that charged side chains localized within the channel lumen favor permeation of ions of opposite sign and inhibit permeation of ions of the same sign.

Comparison with native GlyR channels

Two lines of evidence emerge from our data to imply that adult GlyRs found *in vivo* are composed of α and β subunits. (i) The Hill coefficient for glycine activation of $\alpha1/\beta$ hetero-oligomers expressed in HEK-293 cells roughly corresponds to those values determined for glycine responses in neurons ($n = 1.7-2.7$) (Werman *et al.*, 1968; Lewis *et al.*, 1989; Tokutomi *et al.*, 1989). This is consistent with a stoichiometry of three α plus two β subunits, as suggested earlier for the affinity-purified receptor protein (Langosch *et al.*, 1988). Although our data do not definitely rule out other stoichiometries, the ratio of α to β subunits in recombinant receptors appears to be fixed since the values of main- and subconductance states were similar for each patch examined. (ii) The conductance properties of α/β receptors (44–54 pS main-state) are similar to those of native GlyR, as main-state conductances of 42–48 pS and subconductance levels of 10–14, 18–20 and 27–32 pS have been reported in cultured spinal neurons as well as in neonatal (P2–P3) and adult (P16) tissue slices (Hamill *et al.*, 1983; Bormann *et al.*, 1987; Smith *et al.*, 1989; Takahashi and Momiyama, 1991; Twyman and MacDonald, 1991; Takahashi *et al.*, 1992). This suggests that the predominant form of native GlyRs at these developmental stages is an α/β hetero-oligomer. On the other hand, additional but less frequent conductances were observed in embryonic (E20), neonatal (P2–P3) and adult (P16) spinal slices (79 pS; Takahashi and Momiyama, 1991), as well as in cultured spinal neurons (64 and 93 pS; Smith *et al.*, 1989). A prominent conductance of 94 pS was reported for embryonic (E20) spinal slices (Takahashi *et al.*, 1992). These higher conductance levels are reminiscent of recombinant homo-oligomeric $\alpha1$ and $\alpha2/\alpha3$ GlyRs.

Taken together, these data suggest that: (i) homo-oligomeric $\alpha2$ receptors are exchanged by receptors containing the $\alpha1$ subunit during development and (ii) adult GlyRs are predominantly, but not exclusively, composed of α and β subunits. Our electrophysiological results corroborate a temporal pattern of GlyR isoform expression as originally derived from biochemical (Becker *et al.*, 1988, 1992; Langosch *et al.*, 1988; Hoch *et al.*, 1989) and *in situ* hybridization (Malosio *et al.*, 1991) data.

Materials and methods

Cell transfection

Human embryonic kidney cells (HEK-293 cells, ATCC CRL 1573) were grown on 12 mm coverslips (Thermanox) and transfected as described previously (Sontheimer *et al.*, 1989). The culture medium was MEM medium supplemented with 10% heat-inactivated fetal calf serum. Plasmid DNA was added to subconfluent cell layers using a modified calcium phosphate precipitation technique (Chen and Okayama, 1987). Transfected cells were incubated for ~40 h before electrophysiological experiments. For transfection, the human $\alpha1$ and $\alpha2$ (Grenningloh, 1990a), rat $\alpha3$ (Kuhse *et al.*, 1990) and rat β (Grenningloh *et al.*, 1990b) subunit cDNAs were inserted into the mammalian expression vectors pCIS2 (Gorman *et al.*, 1989) or pRC/CMV (Invitrogen), both of which carry a cytomegalovirus promoter.

Site-directed mutagenesis

The construction of mutants βE290Q, βE297S and βB was described previously (Pribilla *et al.*, 1992). For the other mutants, single-stranded phagemid DNA derived from pRC/CMV was used as template and point mutations introduced using either the Amersham or the BioRad mutagenesis systems. All mutations were verified by dideoxy sequencing. Mutant βB was used as a template to construct mutant βB,E297S. Upon mutating the β subunit, *Xho*I fragments comprising their complete coding regions were subcloned into pCIS2 to ensure identical expression levels for all β mutants. Oligonucleotides used for mutagenesis were: mutant βB/E297S, 5′-TTTGG-GAAGCGACGCTCGGGAGCCGGAGCTCTGTGTGGTCAT-3′; mutant βE290Q,E297S, 5′-TTTGGGAAGCGACGCTGCGAGGGTGGTG-CACTGTGAGGCC-AA-3′; mutant α1G221A, 5′-GCTCGTGTGGCCCT-AGGCATC-3′.

Electrophysiological recording

Electrophysiology was carried out essentially as described previously (Bormann *et al.*, 1987; Feigenspan *et al.*, 1993). Coverslips were placed in a flow chamber mounted on the stage of an inverted microscope. The preparation was continuously perfused (0.5 ml/min) at room temperature (21–25°C) with a solution containing 137 mM NaCl, 5.4 mM KCl, 1.8 mM $CaCl_2$, 1 mM $MgCl_2$, 5 mM HEPES (pH 7.4). The cells were visualized with bright-field optics at 256 × magnification. Membrane currents were recorded from individual cells and from excised membrane patches using the whole-cell and outside-out patch configurations of the patch-clamp technique, respectively (Hamill *et al.*, 1981). Patch pipettes were filled with a solution containing 120 mM CsCl, 20 mM TEA–Cl, 1 mM $CaCl_2$, 2 mM $MgCl_2$, 11 mM EGTA, 10 mM HEPES (pH 7.2). For later analysis, the data were low-pass filtered at 3 kHz (−3 dB, Bessel filter, 24 dB/octave), digitized and stored on hard disk or on a DAT recorder. The sampling rates were 20 and 5 kHz in whole-cell and single-channel experiments, respectively. Glycine was applied in extracellular bath solution to single cells and to excised membrane patches with a fast-application system (Bormann, 1992). The time period of application was in the order of 10 s. For dose–response curves, glycine concentrations ranged from 10 μM to 1 mM. Higher concentrations did not induce larger responses, which indicates saturating conditions. Whole-cell current–voltage (I–V) relationships were obtained by ramping the membrane potential from −70 to 70 mV (100 mV/s). Glycine-activated single-channel currents were analyzed following low-pass filtering at 0.5 or 2.3 kHz (−3 dB, four-pole Bessel filter). The analysis of current amplitude was made by a semi-automatic procedure, where each step change in current was measured on the computer screen by visual inspection using two cursors (Sigworth, 1983). Single-channel current–voltage (i–V) relationships were obtained by measuring 50–100 amplitudes at different membrane potentials. Amplitude histograms were compiled from 500–10000 channel openings measured at −70 mV (bin-width 0.2 pA) and fitted with multiple Gauss functions. Peak amplitudes and relative frequencies of events were derived from the fits and assigned for each patch to the conductance states observed.

Acknowledgements

We thank Drs I.Pribilla and J.Kuhse for providing the plasmid constructs, A.Herbold and G.Heiss-Herzberger for technical assistance, S.Wartha and I.Odenthal for help with the manuscript, C.Fischer for statistical analysis, and Drs V.O'Connor and M.Duggan for critically reading the manuscript. This work was supported by the Deutsche Forschungsgemeinschaft (SFB 169 and Leibniz Programm) and the Fonds der Chemischen Industrie.

References

Akaike,N. and Kaneda,M. (1989) *J. Neurophysiol.*, **62**, 1400–1408.
Becker,C.M., Hoch,W. and Betz,H. (1988) *EMBO J.*, **7**, 3717–3726.
Becker,C.-M., Schmieden,V., Tarroni,P., Strasser,U. and Betz,H. (1992) *Neuron*, **8**, 283–289.
Betz,H. (1992) *Q. Rev. Biophys.*, **25**, 381–394.
Bormann,J. (1991) In Barnard,E.A. and Costa,E. (eds), *Transmitter Amino Acid Receptors: Structures, Transduction and Models for Drug Development*. Thieme, New York, pp. 473–491.
Bormann,J. (1992) In Kettenmann,H. and Grantyn,R. (eds), *Practical Electrophysiological Methods: A Guide for In Vitro Studies in Vertebrate Neurobiology*. Wiley Liss, New York, pp. 136–140.
Bormann,J., Hamill,O.P. and Sakmann,B. (1987) *J. Physiol. (London)*, **385**, 243–286.
Chen,C. and Okayama,H. (1987) *Mol. Cell. Biol.*, **7**, 2745–2751.
Claudio,T., Paulson,H.L., Green,W.N., Ross,A.F., Hartman,D.S. and Hayden,D. (1989) *J. Cell Biol.*, **108**, 2277–2290.
Feigenspan,A., Wässle,H. and Bormann,J. (1993) *Nature*, **361**, 159–162.
Galzi,J.L., Devillers-Thiery,A., Hussy,N., Bertrand,S., Changeux,J.-P. and Bertrand,D. (1992) *Nature*, **359**, 500–505.
Gormann,C.M., Gies,D., McGray,G. and Huang,M. (1989) *Virology*, **171**, 377–385.
Grenningloh,G., Rienitz,A., Schmitt,B., Methfessel,C., Zensen,M., Beyreuther,K., Gundelfinger,E.D. and Betz,H. (1987) *Nature*, **328**, 215–220.
Grenningloh,G., Schmieden,V., Schofield,P.R., Seeburg,P.H., Siddique,T., Mohandas,T.K., Becker,C.-M. and Betz,H. (1990a) *EMBO J.*, **9**, 771–776.
Grenningloh,G., Pribilla,I., Prior,P., Multhaup,G., Beyreuther,K., Taleb,O. and Betz,H. (1990b) *Neuron*, **4**, 963–970.
Hamill,O.P., Marty,A., Neher,E., Sakmann,B. and Sigworth,F.J. (1981) *Pflügers Arch.*, **391**, 85–100.
Hamill,O.P., Bormann,J. and Sakmann,B. (1983) *Nature*, **305**, 805–808.
Hoch,W., Betz,B. and Becker,C.-M. (1989) *Neuron*, **3**, 339–348.
Hurtley,S.M. and Helenius,A. (1989) *Annu. Rev. Cell Biol.*, **5**, 277–307.
Imoto,K., Busch,C., Sakmann,B., Mishina,M., Konno,T., Nakai,J., Bujo,H., Mori,Y., Fukuda,K. and Numa,S. (1988) *Nature*, **335**, 645–648.
Imoto,K., Konno,T., Nakai,J., Wang,F., Mishina,M. and Numa,S. (1991) *FEBS Lett.*, **289**, 193–200.
Kuhse,J., Schmieden,V. and Betz,H. (1990) *J. Biol. Chem.*, **265**, 22317–22320.
Langosch,D., Thomas,L. and Betz,H. (1988) *Proc. Natl Acad. Sci. USA*, **85**, 7394–7398.
Langosch,D., Hartung,K., Grell,E., Bamberg,E. and Betz,H. (1991) *Biochim. Biophys. Acta*, **1063**, 36–44.
Lewis,C.A., Ahmed,Z. and Faber,D.S. (1989) *Neurosci. Lett.*, **96**, 185–190.
Lewis,C.A., Ahmed,Z. and Faber,D.S. (1991) *J. Neurophysiol.*, **66**, 1291–1303.
Malosio,M.-L., Marqueze-Pouey,B., Kuhse,J. and Betz,H. (1991) *EMBO J.*, **10**, 2401–2409.
Pfeiffer,F., Graham,D. and Betz,H. (1982) *J. Biol. Chem.*, **257**, 818–823.
Pribilla,I., Takagi,T., Langosch,D., Bormann,J. and Betz,H. (1992) *EMBO J.*, **11**, 4305–4311.
Schmieden,V., Grenningloh,G., Schofield,P. and Betz,H. (1989) *EMBO J.*, **8**, 695–700.
Sigworth,F.J. (1983) In Sakmann,B. and Neher,E. (eds), *Single-Channel Recording*. Plenum, New York, pp. 301–321.
Smith,S.M., Zorec,R. and McBurney,R.N. (1989) *J. Membrane Biol.*, **108**, 45–52.
Sontheimer,H., Becker,C.-M., Pritchett,D.B., Schofield,P.R., Grenningloh,G., Kettenmann,H., Betz,H. and Seeburg,P.H. (1989) *Neuron*, **2**, 1491–1497.
Takahashi,T. and Momiyama,A. (1991) *Neuron*, **7**, 965–969.
Takahashi,T., Momiyama,A., Hirai,K., Hishinuma,F. and Akagi,H. (1992) *Neuron*, **9**, 1155–1161.
Tokutomi,N., Kaneda,M. and Akaike,N. (1989) *Br. J. Pharmacol.*, **97**,353–360.
Twyman,R.E. and MacDonald,R.L. (1991) *J. Physiol. (London)*, **435**, 303–331.
Verdoorn,T.A., Burnashev,N., Monyer,H., Seeburg,P. and Sakmann,B. (1991) *Science*, **252**, 1715–1718.
Villaroel,A., Herlitze,S., Koenen,M. and Sakmann,B. (1991) *Proc. R. Soc. London Ser. B*, **243**, 69–74.
Werman,R., Davidoff,R.A. and Aprison,M.A. (1968) *Nature*, **214**, 681–683.

Received on May 14, 1993; revised on June 1, 1993